

# Bone marrow-derived mesenchymal stem cells ameliorate sodium nitrite-induced hypoxic brain injury in a rat model

Elham H.A. Ali<sup>1</sup>, Omar A. Ahmed-Farid<sup>2\*</sup>, Amany A. E. Osman<sup>1</sup>

1 Faculty of Women for Art, Sciences and Education, Ain Shams University, Cairo, Egypt

2 National Organization for Drug Control and Research (NODCAR), Giza, Egypt

**How to cite this article:** Ali EHA, Ahmed-Farid OA, Osman AAE (2017) Bone marrow-derived mesenchymal stem cells ameliorate sodium nitrite-induced hypoxic brain injury in a rat model. *Neural Regen Res* 12(12):1990-1999.

## Abstract

Sodium nitrite ( $\text{NaNO}_2$ ) is an inorganic salt used broadly in chemical industry.  $\text{NaNO}_2$  is highly reactive with hemoglobin causing hypoxia. Mesenchymal stem cells (MSCs) are capable of differentiating into a variety of tissue specific cells and MSC therapy is a potential method for improving brain functions. This work aims to investigate the possible therapeutic role of bone marrow-derived MSCs against  $\text{NaNO}_2$  induced hypoxic brain injury. Rats were divided into control group (treated for 3 or 6 weeks), hypoxic (HP) group (subcutaneous injection of 35 mg/kg  $\text{NaNO}_2$  for 3 weeks to induce hypoxic brain injury), HP recovery groups N-2wR and N-3wR (treated with the same dose of  $\text{NaNO}_2$  for 2 and 3 weeks respectively, followed by 4-week or 3-week self-recovery respectively), and MSCs treated groups N-2wSC and N-3wSC (treated with the same dose of  $\text{NaNO}_2$  for 2 and 3 weeks respectively, followed by one injection of  $2 \times 10^6$  MSCs *via* the tail vein in combination with 4 week self-recovery or intravenous injection of  $\text{NaNO}_2$  for 1 week in combination with 3 week self-recovery). The levels of neurotransmitters (norepinephrine, dopamine, serotonin), energy substances (adenosine monophosphate, adenosine diphosphate, adenosine triphosphate), and oxidative stress markers (malondialdehyde, nitric oxide, 8-hydroxy-2'-deoxyguanosine, glutathione reduced form, and oxidized glutathione) in the frontal cortex and midbrain were measured using high performance liquid chromatography. At the same time, hematoxylin-eosin staining was performed to observe the pathological change of the injured brain tissue. Compared with HP group, pathological change of brain tissue was milder, the levels of malondialdehyde, nitric oxide, oxidized glutathione, 8-hydroxy-2'-deoxyguanosine, norepinephrine, serotonin, glutathione reduced form, and adenosine triphosphate in the frontal cortex and midbrain were significantly decreased, and glutathione reduced form/oxidized glutathione and adenosine monophosphate/adenosine triphosphate ratio were significantly increased in the MSCs treated groups. These findings suggest that bone marrow-derived MSCs exhibit neuroprotective effects against  $\text{NaNO}_2$ -induced hypoxic brain injury through exerting anti-oxidative effects and providing energy to the brain.

**Key Words:** nerve regeneration; hypoxia; bone marrow-derived mesenchymal stem cells; sodium nitrite; monoamine neurotransmitter; cell energy; neural regeneration

## Introduction

Oxygen homeostasis is critical for many physiological and developmental processes, and its disturbances have key roles in the pathogenesis of many human diseases, including renal disease (Semenza, 2002). Hypoxia is referred to as a pathological process, in which circulatory hypoxia refers to insufficient blood flow leading to inadequate oxygenation of the tissues, which is also called hypokinetic hypoxia. Sodium nitrite ( $\text{NaNO}_2$ ) is an inorganic salt, soluble in water, which is used in dyes, curing of meat, chemical industry, and colouring agents (Smith, 1967). Unlike the ferrous form of hemoglobin, methemoglobin does not strongly bind with oxygen.  $\text{NaNO}_2$  is highly reactive with hemoglobin causing methemoglobinemia, a condition in which there is a reduction in hemoglobin stability to transmit oxygen leading to hypoxia (Craun et al., 1981; Knobloch et al., 2000). Our bodies require oxygen to metabolize glucose. This process provides energy for the cells. The body reacts to hypoxia with adaptive responses, such as the relaxation of smooth

muscle, angiogenesis, and vasodilatation, thus increasing blood supply to tissues and compensating for the lack of oxygen (Farias et al., 2005). The brain consumes about a fifth of the body's total oxygen supply and requires energy to transmit electrochemical impulses between cells and to maintain the ability of neurons to receive and respond to these signals. Cells of the brain will start to die within a few minutes if they are deprived of oxygen (Fellman and Raivio, 1997). The brain needs a constant supply of oxygen to survive and function. Any interruption in this supply leads to a condition called hypoxia, which can cause brain injury (Roland et al., 1988) and the lack of oxygen leads to the generation of free radicals (Barnham et al., 2004). The brain requires large amounts of oxygen to function; hypoxic damage can often be widespread, cause long-term disabilities, and could lead to cell death (Sataieva and Zadnipyany, 2015). The brain is the target for different stressors because of its high sensitivity to stress-induced degenerative conditions. It is well known that intensive stress response results in the

## \*Correspondence to:

Omar A. Ahmed-Farid, Ph.D.,  
ebntaimya@yahoo.com.

## orcid:

0000-0002-1020-5777

(Omar A. Ahmed-Farid)

doi: 10.4103/1673-5374.221155

Accepted: 2017-11-01

production of reactive oxygen species (ROS), *i.e.*, superoxide anion radical ( $O_2^{\cdot-}$ ), hydroxyl radical ( $HO\cdot$ ), and hydrogen peroxide ( $H_2O_2$ ) that cause lipid peroxidation, especially in membranes and can play an important role in tissue injury (Kovács et al., 1996). There are several studies that are related to the effects of stress on the antioxidant system and induction of lipid peroxidation in the brain of various stress exposure models (Liu et al., 1996).

Sodium nitrite ( $NaNO_2$ ) administration causes dysregulation of inflammation, hypoxia, ischemia, oxidative stress, and impaired metabolic energy, which finally exacerbate organ damage, including brain injury (El-Sheikh and Khalil, 2011; Salama et al., 2013; Aita and Mohammed, 2014). Sodium nitrite binding to oxyhemoglobin displaces the bound oxygen and yields methemoglobin, hydrogen peroxide, and nitrogen dioxide in a free radical chain initiation step (Kosaka et al., 1979). The nitrogen dioxide oxidizes ferrous hemoglobin to methemoglobin, whereas hydrogen peroxide oxidizes methemoglobin to the ferryl hemoglobin radical. The reaction of ferryl hemoglobin with nitrite also produces methemoglobin and nitrogen dioxide (Spagnuolo et al., 1987). This prevents oxygen binding to hemoglobin, reducing the oxygen carrying capacity of the blood, leading to hypoxia. Lan and co-workers showed that hypoxia generated oxidative stress in the rat brain by decreasing the activities of antioxidant enzymes while increasing the lipid peroxidation levels (Lan et al., 2016). Previous studies indicated that oxidative stress is an early feature after exposure to hypoxia and any degree of hypoxia will affect the brain function (Blomgren et al., 2001). Recent studies have shown that mesenchymal stem cells (MSCs) are capable of differentiating into a variety of tissue specific cells and MSC therapy is a potential method for improving brain functions (Moisan et al., 2012). Recently, advancements have been achieved in use of stem cells to successfully treat neurological conditions such as Parkinson's disease, spinal cord injury, and amyotrophic lateral sclerosis (Kim and de Vellis, 2009). In hypoxic brain injury, MSCs secrete many neurotrophic factors such as brain derived neurotrophic factor and vascular endothelial growth factor, to develop neuronal and vascular markers, and repair the injured brain (Lee et al., 2010). This study aimed to investigate the ameliorative and therapeutic effect of bone marrow-derived MSCs on hypoxic brain injury induced by  $NaNO_2$  at different duration levels, the effects of hypoxia on the histological damage of the cerebral cortex, the role of the bone marrow-derived MSC pathway in metabolic dysfunction-induced oxidative stress, and the development of the hypoxic brain.

## Materials and Methods

### Experimental animals

Male Wistar rats, aged 3 months, weighing 200–220 g, were used in this study. Eighty-four rats were obtained from the Laboratory Animal Center of Ain Shams Hospital, Egypt. The rats were raised in plastic cages, with 12 rats in each cage, in a 12-hour dark/light environment at  $25 \pm 2^\circ C$ . A commercial pelleted diet was used during the experiment. The rats were acclimatized to the laboratory environment for one week before the beginning of the experiment. The experimental protocols and procedures were performed

according to Ain Shams University authorities, which were in accordance with the U.K. Animals (Scientific Procedures) Act, 1986 and associated guidelines.

### Isolation, propagation, identification, and labelling of bone marrow-derived MSCs from rats

Bone marrow cells were collected from six rats and cultured according to a previously described procedure (Alhadlaq and Mao, 2004). These cells were known as MSCs according to their morphology, adherence, and their ability to differentiate into osteocytes (Jaiswal et al., 1997) and chondrocytes (Seo et al., 2009). PKH26, a red fluorochrome, was used to label the undifferentiated MSCs while maintaining their biological and proliferating potential (Sohni and Verfaillie, 2013) as stated by the manufacturer's reference (Sigma, Saint Louis, Missouri, USA). Cells were intravenously injected into the tail vein of rats. One month later, the homing of injected MSCs in the brain tissue, *i.e.*, PKH26-stained cells, was detected by a fluorescence microscope (LABOMED LX400 SERIES, USA). Inflammation-directed MSC homing involved numerous vital cell trafficking-related molecules such as chemokines, matrix metalloproteinases, and adhesion molecules (Sohni and Verfaillie, 2013).

### Experimental design

The animals were randomly divided into seven groups, with 12 rats in each group.

- Control group 1 (C1): Dorsal subcutaneous injection of distilled water (0.1 mL/100 g body weight) for 21 days, followed by sacrifice by decapitation.
- Control group 2 (C2): Dorsal subcutaneous injection of distilled water (0.1 mL/100 g body weight) for 14 days, followed by no intervention for 4 weeks.
- Hypoxic group (HP group): Subcutaneous injection of sodium nitrite ( $NaNO_2$ ) (35 mg/kg/d; Sigma St. Louis, MO, USA, as a pure white powder (assay  $\geq 99\%$ ) (Bhanumathy et al., 2010) for 21 days, to induce chemical hypoxia
- N-2wR group: Subcutaneous injection of  $NaNO_2$  (35 mg/kg/d) for 15 days, followed by no intervention for 28 days.
- N-3wR group: Subcutaneous injection of  $NaNO_2$  (35 mg/kg/d) for 21 days, followed by no intervention for 21 days.
- N-2wSC group: Subcutaneous injection of  $NaNO_2$  (35 mg/kg/d) for 15 days, followed by one intravenous injection of MSCs *via* the tail vein ( $2 \times 10^6$  cells/rat) and no injection for 28 days.
- N-3wSC group: Subcutaneous injection of  $NaNO_2$  (35 mg/kg/d) for 15 days, followed by one intravenous injection of MSCs ( $2 \times 10^6$  cells/rat), 7-day  $NaNO_2$  injection, and 21-day no intervention.

The total time for the experiment was 3 weeks for the C1 and HP groups, and 6 weeks for the rest of the groups as shown in **Figure 1**.

### Biochemical samples

After experiments, the rats were sacrificed by rapid decapitation 24 hours after the last dose. The brains were dissected for determination of the following. Six brains from each group (frontal cortex "Cor" and midbrain "mb") were homogenized in 75% methanol of high-performance liquid chromatogra-

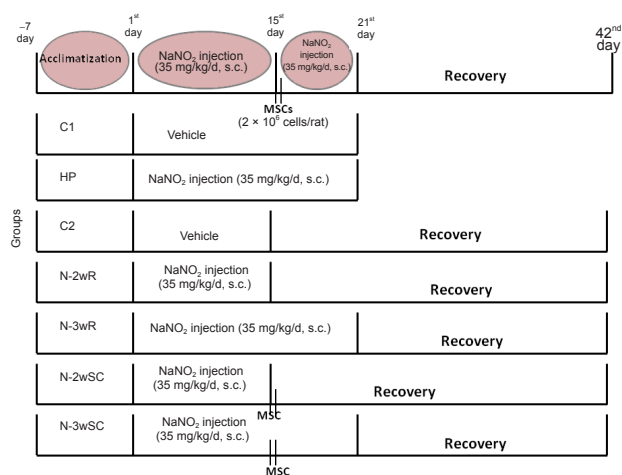


**Figure 1** Schematic diagram for the experimental design

phy (HPLC) grade for determining the levels of monoamines (norepinephrine (NE), dopamine (DA), serotonin (5-HT), adenosine monophosphate (AMP), adenosine diphosphate (ADP), and adenosine triphosphate (ATP) as well as AMP/ATP and ADP/ATP ratios. The remaining six brains from each group were cut longitudinally into two parts. The cortex and midbrain of one part were homogenized in phosphate buffer saline (pH 7.4), and used for determining the levels of glutathione reduced form (GSH), oxidized glutathione (GSSG), malondialdehyde (MDA), total nitric oxide (NO), and 8-hydroxy-2-deoxyguanosine (8-OHdG). The other part of each remaining brain in each group was used for histological and immunohistochemical studies.

### HPLC determination

The cortex and midbrain tissues were weighed and homogenized in 10% (w/v) 75% methanol of HPLC grade or phosphate buffer solution. The homogenized tissue was centrifuged and the supernatant was used for HPLC-UV analysis. The HPLC device used was Agilent HP 1200 series (USA). It included a column oven, quaternary pump, Rheodyne injector, 20- $\mu$ L loop, and variable wavelength UV detector. The energy carriers, monoamines, malondialdehyde (MDA), nitric oxide (NO), 8-OHdG, and reduced/oxidized glutathione standards, used by high-performance liquid chromatography (HPLC) techniques, were also purchased from Sigma (St. Louis, MO, USA), with high purity, and all were of HPLC grade.

For MDA, Supelcosil C18 (5  $\mu$ m particle and 8 nm pore size) (250  $\times$  4.5 mm ID) analytical column was used. The mobile phase was 30 mmol potassium dihydrogen phosphate – methanol of HPLC grade (65–35%  $H_3PO_4$ , pH 4), with a flow rate of 1.5 mL/min and wave length of 250 nm (Karatas et al., 2002; Karatepe, 2004). For reduced and oxidized glutathione (GSH and GSSG), the analytical column was a  $\mu$ -Bondapak sodium (15 cm  $\times$  3.9 mm). The mobile phase was 25 mmol sodium dihydrogen phosphate containing 5 mmol tetra-butyl ammonium phosphate and methanol (87%: 13%  $H_3PO_4$ , pH 3.5), with a flow rate of 1 mL/min and wave-length adjusted at 190 nm (Jayatilleke and Shaw 1993). Nitric oxide (mM) was determined as the ratio of nitrites/nitrate according to the method of Papadoyannis et al. (1999).

An anion exchange PRP X-100 Hamilton, 150  $\times$  4.1 mm by 10 mm analytical column was used and the mobile phase was a mixture of 0.1 M sodium chloride – methanol (45:55, v/v), with a flow rate of 2 mL/min and wavelength of 230 nm. 8-OHdG was determined using the method of Lodovici et al. (1997). For chromatographic separation, C18 reverse phase column was used in series (Supelco, 5  $\mu$ m, I.D. 0.46  $\times$  25 cm); the eluting solution was  $H_2O/CH_2OH$  (85:15 v/v) with 50 mM  $KH_2PO_4$ , pH 5.5, at a flow rate of 0.68 mL/min. The wavelength of UV detector was set at 245 nm. To detect cell energy (AMP, ADP, and ATP) contents, samples were injected into the system which consisted of an analytical column Nucleosil C-18 (15  $\times$  0.4 cm). The mobile phase for the adenine nucleotides was 50 mM potassium phosphate and 1% methanol (v/v) at pH 5.5 with a flow rate of 1 mL/min, and the wavelength of UV detector was set at 210 nm (Teerlink et al., 1993). To determine monoamines, the sample was immediately extracted from the trace elements and lipids using a solid phase extraction CHROMABOND column (NH<sub>2</sub> phase cat. No. 730031). The sample was then injected directly into a 150  $\times$  54.6 mm, 5  $\mu$ m AQUA column, purchased from Phenomenex, USA under the following conditions: mobile phase 20 mM potassium phosphate, pH 2.7, flow rate 1.5 mL/min, UV wavelength 290 nm (Pagel et al., 2000).

### Histological and immunohistochemical assays

The rat brains were carefully excised and fixed in Bouin's fixative for histological study. After fixation, the brains were processed in ascending grades of ethyl alcohol, cleared in xylol, and implanted in paraffin wax at 60°C. Serialized 5–6  $\mu$ m sections were then cut by a Cambridge Rocking Microtome (Cat. No. 52111, London) and affixed on slides. The sections on the slides were stained with hematoxylin and eosin (Drury and Wallington, 1980). Expression of proliferating cell nuclear antigen (PCNA) protein in brain tissue was identified with immunohistochemical staining for PCNA specific for rats using the avidin-biotin peroxidase complex ABC technique (Bancroft et al., 1994) for 10 minutes for the primary antibody and 15 minutes for secondary antibody at room temperature (25°C). The site of antibody binding was visualized after adding (diaminobenzidine) chromogen, which is converted into a brown precipitate by peroxidase, and PCNA-positive cells demonstrated brown nuclear deposits. Image analysis was performed by ImmunoRatio Program (version: 1.0C), Institute of Biomedical Technology, University of Tampere, Finland. The percentage of PCNA-positive cells stained brown, and the percentage of PCNA-stained nuclear area over total nuclear area (labeling index) were calculated.

### Statistical analysis

Data were statistically analyzed using SPSS 18.0 software (SPSS, Chicago, IL, USA) and are expressed as the mean  $\pm$  SE. One-way analysis of variance was used for comparison among multiple groups. *Post hoc* test (Bonferroni test) was used for comparisons between groups.

## Results

### Biochemical measurements

There was no significant difference in any biochemical

**Table 1 Levels of MDA (nmol/g wet tissue), NO ( $\mu\text{mol/g}$  wet tissue), and 8-OHdG (pg/g wet tissue) in rat cortex and midbrain in each group**

Group	Brain cortex			Midbrain		
	MDA	NO	8-OHdG	MDA	NO	8-OHdG
C1	5.71 $\pm$ 0.09	0.33 $\pm$ 0.01	231.9 $\pm$ 14.6	3.54 $\pm$ 0.17	0.25 $\pm$ 0.02	169.0 $\pm$ 5.6
C2	6.33 $\pm$ 0.29	0.34 $\pm$ 0.01	232.3 $\pm$ 12.2	3.45 $\pm$ 0.12	0.25 $\pm$ 0.01	168.4 $\pm$ 6.4
HP	8.10 $\pm$ 0.34 <sup>a</sup>	0.65 $\pm$ 0.04 <sup>a</sup>	344.4 $\pm$ 13.1 <sup>a</sup>	4.98 $\pm$ 0.22 <sup>a</sup>	0.41 $\pm$ 0.02 <sup>a</sup>	228.2 $\pm$ 6.4 <sup>a</sup>
N-2wR	7.82 $\pm$ 0.20 <sup>a</sup>	0.53 $\pm$ 0.05 <sup>ab</sup>	299.7 $\pm$ 10.8 <sup>ab</sup>	4.31 $\pm$ 0.10 <sup>ab</sup>	0.34 $\pm$ 0.02 <sup>ab</sup>	194.1 $\pm$ 6.1 <sup>ab</sup>
N-3wR	8.00 $\pm$ 0.15 <sup>a</sup>	0.57 $\pm$ 0.03 <sup>a</sup>	303.9 $\pm$ 12.4 <sup>ab</sup>	4.56 $\pm$ 0.06 <sup>a</sup>	0.37 $\pm$ 0.03 <sup>a</sup>	199.0 $\pm$ 3.5 <sup>ab</sup>
N-2wSC	6.22 $\pm$ 0.23 <sup>bcd</sup>	0.40 $\pm$ 0.02 <sup>bcd</sup>	260.1 $\pm$ 11.1 <sup>bcd</sup>	3.41 $\pm$ 0.22 <sup>bcd</sup>	0.30 $\pm$ 0.02 <sup>bd</sup>	178.2 $\pm$ 4.8 <sup>bd</sup>
N-3wSC	6.71 $\pm$ 0.25 <sup>bcd</sup>	0.45 $\pm$ 0.02 <sup>abd</sup>	265.1 $\pm$ 9.0 <sup>bcd</sup>	3.78 $\pm$ 0.09 <sup>bcd</sup>	0.33 $\pm$ 0.01 <sup>ab</sup>	207.6 $\pm$ 8.7 <sup>abe</sup>

Values are expressed as the mean  $\pm$  SE across six rats in each group. One-way analysis of variance and Bonferroni correction were used. <sup>a</sup> $P < 0.05$ , vs. control groups; <sup>b</sup> $P < 0.05$ , vs. HP group; <sup>c</sup> $P < 0.05$ , vs. N-2wR group; <sup>d</sup> $P < 0.05$ , vs. N-2wSC group; <sup>e</sup> $P < 0.05$ , vs. N-3wSC group. Control group 1 (C1): Dorsal subcutaneous injection of distilled water (0.1 mL/100 g body weight) for 21 days, followed by sacrifice by decapitation. Control group 2 (C2): Dorsal subcutaneous injection of distilled water (0.1 mL/100 g body weight) for 14 days, followed by no intervention for 4 weeks. Hypoxic (HP) group: Subcutaneous injection of NaNO<sub>2</sub> (35 mg/kg/d) for 21 days. N-2wR and N-3wR groups: subcutaneous injection of NaNO<sub>2</sub> (35 mg/kg/d) for 15 and 21 days respectively, followed by no intervention for 28 and 21 days respectively. N-2wSC group: Subcutaneous injection of NaNO<sub>2</sub> (35 mg/kg/d) for 15 days, followed by one intravenous injection of MSCs via the tail vein ( $2 \times 10^6$  cells/rat) and no injection for 28 days. N-3wSC group: Subcutaneous injection of NaNO<sub>2</sub> (35 mg/kg/d) for 15 days, followed by one intravenous injection of MSCs ( $2 \times 10^6$  cells/rat), 7-day NaNO<sub>2</sub> injection, and 21-day no intervention. MDA: Malondialdehyde; NO: nitric oxide; 8-OHdG: 8-hydroxy-2-deoxyguanosine.

**Table 2 Levels of GSH, GSSG ( $\mu\text{mol/g}$  wet tissue), GSH/GSSG (%), and oxidized GSSG ratio (%) in rat cortex and midbrain in each group**

Group	Cortex				Midbrain			
	GSH	GSSG	GSH/GSSG ratio	Oxidized GSSG ratio	GSH	GSSG	GSH/GSSG ratio	Oxidized GSSG ratio
C1	14.6 $\pm$ 0.15	0.73 $\pm$ 0.03	21.35 $\pm$ 0.50	0.08 $\pm$ 0.002	14.2 $\pm$ 0.41	0.69 $\pm$ 0.02	22.1 $\pm$ 1.28	0.08 $\pm$ 0.006
C2	14.3 $\pm$ 0.13	0.70 $\pm$ 0.02	20.52 $\pm$ 0.63	0.09 $\pm$ 0.003	13.3 $\pm$ 0.23	0.64 $\pm$ 0.04	21.09 $\pm$ 1.38	0.09 $\pm$ 0.005
HP	10.7 $\pm$ 0.20 <sup>a</sup>	1.46 $\pm$ 0.17 <sup>a</sup>	8.06 $\pm$ 1.31 <sup>a</sup>	0.21 $\pm$ 0.023 <sup>a</sup>	9.8 $\pm$ 0.27 <sup>a</sup>	1.50 $\pm$ 0.15 <sup>a</sup>	6.88 $\pm$ 0.61 <sup>a</sup>	0.20 $\pm$ 0.009 <sup>a</sup>
N-2wR	11.6 $\pm$ 0.19 <sup>ab</sup>	0.89 $\pm$ 0.08 <sup>b</sup>	13.57 $\pm$ 1.32 <sup>ab</sup>	0.14 $\pm$ 0.010 <sup>ab</sup>	10.9 $\pm$ 0.26 <sup>ab</sup>	1.01 $\pm$ 0.05 <sup>ab</sup>	10.91 $\pm$ 0.48 <sup>ab</sup>	0.16 $\pm$ 0.006 <sup>ab</sup>
N-3wR	11.9 $\pm$ 0.17 <sup>ab</sup>	1.17 $\pm$ 0.04 <sup>abc</sup>	10.16 $\pm$ 0.37 <sup>ac</sup>	0.17 $\pm$ 0.005 <sup>ab</sup>	10.1 $\pm$ 0.30 <sup>a</sup>	1.33 $\pm$ 0.15 <sup>ac</sup>	9.22 $\pm$ 1.06 <sup>a</sup>	0.18 $\pm$ 0.008 <sup>ab</sup>
N-2wSC	12.1 $\pm$ 0.29 <sup>ab</sup>	0.82 $\pm$ 0.03 <sup>bd</sup>	14.89 $\pm$ 0.76 <sup>abd</sup>	0.12 $\pm$ 0.004 <sup>bd</sup>	11.7 $\pm$ 0.45 <sup>abd</sup>	0.84 $\pm$ 0.04 <sup>bd</sup>	14.84 $\pm$ 0.88 <sup>abcd</sup>	0.13 $\pm$ 0.006 <sup>abcd</sup>
N-3wSC	12.8 $\pm$ 0.33 <sup>abcde</sup>	0.92 $\pm$ 0.05 <sup>bd</sup>	14.00 $\pm$ 0.79 <sup>abd</sup>	0.13 $\pm$ 0.006 <sup>abd</sup>	11.3 $\pm$ 0.47 <sup>abd</sup>	0.95 $\pm$ 0.04 <sup>abd</sup>	13.68 $\pm$ 1.18 <sup>abd</sup>	0.15 $\pm$ 0.008 <sup>abd</sup>

All values are expressed as the mean  $\pm$  SE across six rats in each group. One-way analysis of variance and Bonferroni correction were used. <sup>a</sup> $P < 0.05$ , vs. C1 and C2 groups; <sup>b</sup> $P < 0.05$ , vs. HP group; <sup>c</sup> $P < 0.05$ , vs. N-2wR group; <sup>d</sup> $P < 0.05$ , vs. N-2wSC group; <sup>e</sup> $P < 0.05$ , vs. N-3wSC group. Control group 1 (C1): Dorsal subcutaneous injection of distilled water (0.1 mL/100 g body weight) for 21 days, followed by sacrifice by decapitation. Control group 2 (C2): Dorsal subcutaneous injection of distilled water (0.1 mL/100 g body weight) for 14 days, followed by no intervention for 4 weeks. Hypoxic (HP) group: Subcutaneous injection of NaNO<sub>2</sub> (35 mg/kg/d) for 21 days. N-2wR and N-3wR groups: subcutaneous injection of NaNO<sub>2</sub> (35 mg/kg/d) for 15 and 21 days respectively, followed by no intervention for 28 and 21 days respectively. N-2wSC group: Subcutaneous injection of NaNO<sub>2</sub> (35 mg/kg/d) for 15 days, followed by one intravenous injection of MSCs via the tail vein ( $2 \times 10^6$  cells/rat) and no injection for 28 days. N-3wSC group: Subcutaneous injection of NaNO<sub>2</sub> (35 mg/kg/d) for 15 days, followed by one intravenous injection of MSCs ( $2 \times 10^6$  cells/rat), 7-day NaNO<sub>2</sub> injection, and 21-day no intervention. GSH: Total glutathione; GSSG: oxidized glutathione.

measurement between C1 and C2 groups. As shown in **Table 1**, MDA, NO, and 8-OHdG levels in the rat cortex and midbrain were significantly increased in the HP, N-2wR, and N-3wR groups than in the control groups ( $P < 0.05$ ), with the exception of 8-OHdG level in the HP group. The levels of oxidative stress markers especially MDA, NO, and 8-OHdG in the rat cortex and midbrain were significantly increased in the N-2wSC group than in the HP, N-2wR, and N-3wR groups. The level of 8-OHdG in the rat midbrain in the N-3wSC group was significantly increased than that in the control group.

As shown in **Table 2**, GSH level in the rat cortex and midbrain and the GSH/GSSG ratio were significantly decreased in the HP, N-2wR, and N-3wR groups than in the C1 and C2 groups ( $P < 0.05$ ). The GSSG and oxidized GSSG ratio were significantly increased in the HP and N-3wR groups than in the C1 and C2 groups. Moreover, the oxidized GSSG ratio in

the rat cortex and midbrain was significantly increased in the N-2wR group than in the C1 and C2 groups. The GSH level and GSH/GSSG ratio in the rat cortex and midbrain were significantly decreased in the N-2wSC and N-3wSC groups than in the C1 and C2 groups. The oxidized GSSG ratio in the rat midbrain was significantly decreased in the N-2wSC and N-3wSC groups than in the C1 and C2 groups. The oxidized GSSG ratio in the rat cortex was significantly decreased in the N-2wSC group than in the C1 and C2 groups.

As shown in **Table 3**, ATP level in the rat cortex and midbrain was significantly decreased in the HP, N-2wR, and N-3wR groups than in the C1 and C2 groups ( $P < 0.05$ ). AMP/ATP and ADP/ATP ratios in the rat cortex and midbrain were significantly increased in the HP, N-2wR, and N-3wR group, except ADP/ATP ratio in the rat cortex in the N-2wR group, than in the C1 and C2 groups. However, ATP level, AMP/ATP and ADP/ATP ratios in the rat cortex and

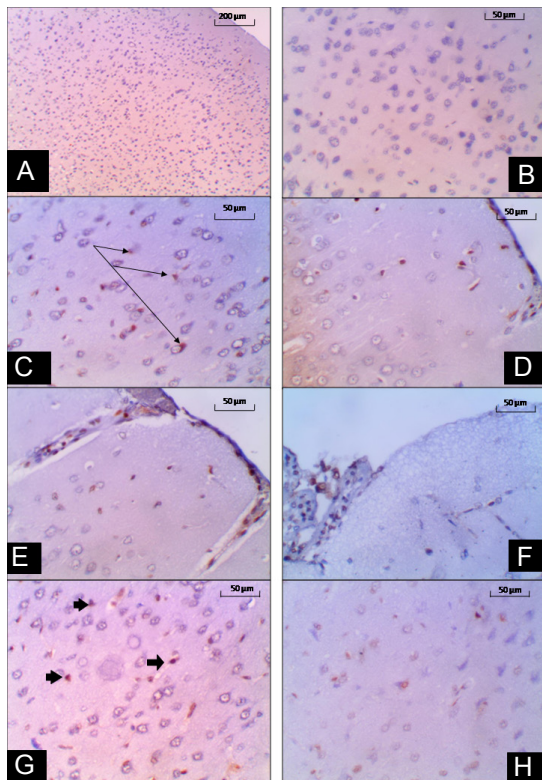
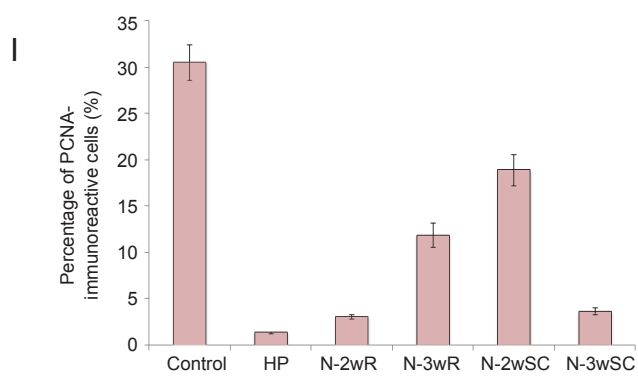


**Figure 2** Proliferating cell nuclear antigen (PCNA)-immunoreactive cells in the cerebral cortex from hypoxic/ischemic brain injury rats following MSCs injection.



(A–H) Representative micrographs of immunohistochemistry for PCNA. (A, B) Control rats: Showing a few PCNA immunoreactive cells in the cerebral cortex. (C) N-2wR group: Showing markedly distributed PCNA-immunoreactive cells. (D) N-3wR group: Showing few PCNA-immunoreactive cells. (E, F) Hypoxic group: Showing few PCNA-immunoreactive cells in the pia matter and nerve plexus. (G) N-2wSC group: PCNA-immunoreactive cells well distributed in the cerebral cortex, molecular layer, external granular layer, and particularly in blood capillary lining epithelial tissue. (H) N-3wSC group: Wide distribution of PCNA-immunoreactive cells throughout the cerebral cortex. The arrows showed PCNA-immunoreactive cells as brown nuclear deposits. Scale bars: 200  $\mu$ m in A, 50  $\mu$ m in B–H. (I) Quantification of PCNA-immunoreactive cells (%). Control group 1 (C1): Dorsal subcutaneous injection of distilled water (0.1 mL/100 g body weight) for 21 days, followed by sacrifice by decapitation. Control group 2 (C2): Dorsal subcutaneous injection of distilled water (0.1 mL/100 g body weight) for 14 days, followed by no intervention for 4 weeks. Hypoxic (HP) group: Subcutaneous injection of NaNO<sub>2</sub> (35 mg/kg/d) for 21 days. N-2wR and N-3wR groups: subcutaneous injection of NaNO<sub>2</sub> (35 mg/kg/d) for 15 and 21 days respectively, followed by no intervention for 28 and 21 days respectively. N-2wSC group: Subcutaneous injection of NaNO<sub>2</sub> (35 mg/kg/d) for 15 days, followed by one intravenous injection of MSCs *via* the tail vein ( $2 \times 10^6$  cells/rat) and no injection for 28 days. N-3wSC group: Subcutaneous injection of NaNO<sub>2</sub> (35 mg/kg/d) for 15 days, followed by one intravenous injection of MSCs ( $2 \times 10^6$  cells/rat), 7-day NaNO<sub>2</sub> injection, and 21-day no intervention.

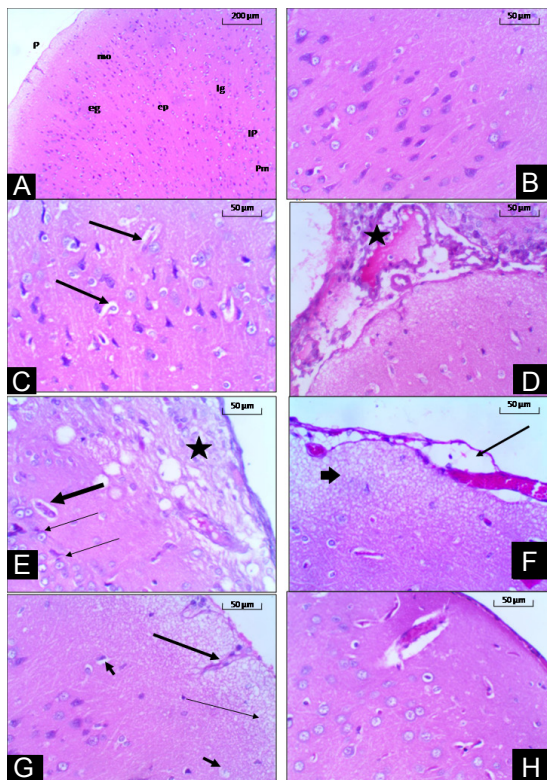


**Figure 3** Representative micrographs of hematoxylin-eosin-stained cerebral cortex sections from rats with hypoxic/ischemic brain injury following BMMSCs injection.

(A) Control group: The molecular layer (mo) was covered with pia matter (P), external granular layer (eg), external pyramidal layer (ep), internal granular layer (Ig), internal pyramidal layer (Ip), and polymorphic layer (pm). (B) N-2wR group: Ameliorative cerebral tissue patterns were observed, congestion of capillary blood vessels still persisted with fibrosis of the epithelial layer and presence of patches as areas devoid of staining quality within cortical tissues. (C) N-3wR group: unstained areas around some cells (thick arrow), and slightly ameliorative area in the rest of cortical cells. (D–F) Hypoxic (HP) group: Lymphocytic inflammatory and apoptotic appearance with hyaline material around pia matter and hemorrhage (star) (D); loss of plexus and necrotic area (star) with pyknotic nuclei (thin arrows), widely distributed large vacuoles, and dilated capillary blood vessels (thick arrow) (E); ruptured pia mater, congestion of peripheral capillary blood vessels (arrow), loss of plexus nerve fibers, and a large number of small cytoplasm vacuoles (head) (F). (G) N-2wSC group: cerebral layer cells restored partially to the normal, invaded capillary blood vessels (long thick arrow), unstained area around some cells (short arrow), and moderate loss of plexus (thin arrow). (H) N-3wSC group: Ameliorative cerebral tissue was observed, but capillary blood vessels were dilated, pia mater layer cells invaded in the molecular layer. Scale bars: 200  $\mu$ m in A, 50  $\mu$ m in B–H. Control group: Dorsal subcutaneous injection of distilled water (0.1 mL/100 g body weight); HP group: Subcutaneous injection of NaNO<sub>2</sub> (35 mg/kg/d) for 21 days; N-2wR and N-3wR groups: subcutaneous injection of NaNO<sub>2</sub> (35 mg/kg/d) for 15 and 21 days respectively, followed by no intervention for 28 and 21 days respectively; N-2wSC group: Subcutaneous injection of NaNO<sub>2</sub> (35 mg/kg/d) for 15 days, followed by one intravenous injection of MSCs *via* the tail vein ( $2 \times 10^6$  cells/rat) and no injection for 28 days; N-3wSC group: Subcutaneous injection of NaNO<sub>2</sub> (35 mg/kg/d) for 15 days, followed by one intravenous injection of MSCs ( $2 \times 10^6$  cells/rat), 7-day NaNO<sub>2</sub> injection, and 21-day no intervention.

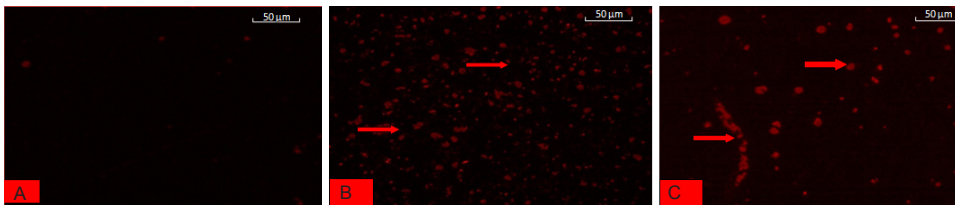


**Figure 4** Representative fluorescence micrographs of cerebral cortex from hypoxic brain injury rats following MSCs injection showing the homing of MSCs by PKH26 dye.

(A) Control group: Absence of MSCs labeled by PKH26 dye. (B) N-2wSC group: Labeling of MSCs with PKH26 dye. MSCs were detected in all the cerebral cell layers, confirming that these cells homed into the cerebral cortex region. (C) N-3wSC group: MSCs were detected in the brain tissues, confirming that these cells homed into the cerebral tissue, but they were less compared with other groups. Scale bars: 50 µm. Control group: Dorsal subcutaneous injection of distilled water (0.1 mL/100 g body weight); N-2wSC group: Subcutaneous injection of NaNO<sub>2</sub> (35 mg/kg/d) for 15 days, followed by one intravenous injection of MSCs *via* the tail vein ( $2 \times 10^6$  cells/rat) and no injection for 28 days; N-3wSC group: Subcutaneous injection of NaNO<sub>2</sub> (35 mg/kg/d) for 15 days, followed by one intravenous injection of MSCs ( $2 \times 10^6$  cells/rat), 7-day NaNO<sub>2</sub> injection, and 21-day no intervention.

midbrain were significantly increased in the N-2wSC and N-3wSC groups than in the HP, N-2wR, and N-3wR groups, although most measurements were better in the N-2wSC group than in the N-3wSC group.

As shown in **Table 4**, NE and 5-HT levels in the rat cortex and midbrain were significantly increased, and dopamine level in the rat cortex was significantly decreased in the HP group, than in the C1 and C2 groups ( $P < 0.05$ ). 5-HT level in the rat cortex and midbrain was significantly increased in the N-2wR and N-3wR group than in the C1 and C2 groups. Dopamine level in the rat cortex and midbrain was significantly decreased in the N-2wR and N-3wR groups than in the C1 and C2 groups ( $P < 0.05$ ). Dopamine level in the rat cortex and midbrain was significantly decreased in the N-3wSC group than in the C1 and C2 groups ( $P < 0.05$ ).

#### Immunohistochemical and histological assessments of rat cerebral cortex

Immunohistochemical assessment of rat cerebral cortex: Very few PCNA-immunoreactive cells were observed in the cerebral cortex of control rats (**Figure 2A, B**). PCNA-immunoreactive cells were mainly distributed in the molecular layer, external granular, and unsurprisingly in blood capillaries lining the epithelial tissue in the rat brain (cerebral cortex) treated with NaNO<sub>2</sub> for 15 days and left for recovery (N-2wR). In the N-2wR and N-3wR groups, a large number of PCNA-immunoreactive cells were observed in the hemorrhagic focus in the pia mater of the cerebral cortex (**Figure 2C**). PCNA-immunoreactive cells were rarely observed in the pia mater and nerve plexus and they were absent in the rest of tissue sections of hypoxic cerebral cortex treated with NaNO<sub>2</sub> for 21 days (N-3wR) (**Figure 2D**). After treatment with NaNO<sub>2</sub> for 21 days (HP group), PCNA-immunoreactive cells were rarely observed in the pia mater region and nerve plexus and they were absent in the rest of tissue sections of hypoxic cerebral cortex (**Figure 2E, F**). The positive effect of stem cell implantation was found in the N-2wSC group. Immunohistochemical staining showed that PCNA-immunoreactive cells were widely illustrated in the molecular layer, external granular, and obviously in the blood capillary lining the epithelial tissue (**Figure 2G**). In the N-3wSC group, PCNA-immunoreactive cells were distributed in the molecular layer, external pyramidal layer, and internal granular layer (**Figure 2H**). The percentage of PCNA-immunoreactive cells is shown in **Figure 2I**. The percentage of PCNA-immunoreactive cells was 30.5%, 1.4%,

3.1%, 11.9%, 18.9% and 3.7% respectively in the control, HP, N-2wR, N-3wR, N-2wSC, and N-3wSC groups, respectively.

Histological assessment of rat cerebral cortex by microscopy: in the control group, the molecular layer was covered with pia matter, external granular layer, external pyramidal layer, internal granular layer, internal pyramidal layer, and polymorphic layer (**Figure 3A**). In the N-2wR group, ameliorative cerebral tissue patterns were observed, congestion of capillary blood vessels still persisted with fibrosis of the epithelial layer and presence of patches as areas devoid of staining quality within cortical tissues (**Figure 3B**). Moreover, unstained areas around shrunken cells were seen in the N-3wR group (**Figure 3C**). In the HP group, capillary blood vessels were dilated, lymphocytic inflammatory cells, thinner pia mater with hemorrhagic changes (**Figure 3D**), loss of plexus, necrotic area with pyknotic nuclei, and widely distributed large vacuoles were observed (**Figure 3E**). Ruptured pia mater and loss of normal cortical layer cells were also evident (**Figure 3F**). Stem cell (MSCs) therapy was introduced to repair the developing capillary damage in the brain and epithelial derived cells. In the N-2wSC group, more ameliorative cerebral tissue was observed, and cells in the cerebral cortex was near to normal (**Figure 3G**). In the N-3wSC group, ameliorative cerebral tissue was observed, but but capillary blood vessels were dilated, pia mater layer cells invaded in the molecular layer (**Figure 3H**).

#### Homing efficiency

In the cerebral cortex of control rats, a few cells homed (**Figure 4A**). In the N-2wSC group, PKH26 fluorescent dye-labeled MSCs were observed in all cerebral cell layers, confirming that these labelled cells homed into the cerebral cortex (**Figure 4B**). In the N-3wSC group, less fluorescent dye was detected in the hypoxic rat brain and stem cells than in the prior groups (**Figure 4C**).

#### Discussion

In this study, we demonstrated that MSCs can significantly alleviate oxidation and neuronal damage after hypoxic brain injury induced by NaNO<sub>2</sub> administered for 2 and 3 weeks. Results showed that levels of MDA, NO, 8-OHdG and GSSG, as well as oxidized GSSG ratio were increased, and GSH level and GSH/GSSG ratio decreased after 2- or 3-week NaNO<sub>2</sub> administration. These findings confirm that MSCs can diminish antioxidant defence. This improvement may

**Table 3 Levels of ATP ( $\mu\text{g/g}$  wet tissue), AMP/ATP ratio, and ADP/ATP ratio in the rat cortex and midbrain**

Group	Cortex			Midbrain		
	ATP	AMP/ATP	ADP/ATP	ATP	AMP/ATP	ADP/ATP
C1	38.03 $\pm$ 2.37	0.22 $\pm$ 0.01	0.35 $\pm$ 0.01	34.45 $\pm$ 0.66	0.02 $\pm$ 0.01	0.34 $\pm$ 0.03
C2	39.31 $\pm$ 2.05	0.21 $\pm$ 0.03	0.33 $\pm$ 0.05	33.40 $\pm$ 0.94	0.20 $\pm$ 0.01	0.35 $\pm$ 0.02
HP	20.96 $\pm$ 1.08 <sup>a</sup>	0.40 $\pm$ 0.02 <sup>a</sup>	1.02 $\pm$ 0.09 <sup>a</sup>	21.47 $\pm$ 1.53 <sup>a</sup>	0.44 $\pm$ 0.03 <sup>a</sup>	0.72 $\pm$ 0.06 <sup>a</sup>
N-2wR	20.75 $\pm$ 0.57 <sup>a</sup>	0.35 $\pm$ 0.02 <sup>a</sup>	0.58 $\pm$ 0.05 <sup>ab</sup>	24.47 $\pm$ 1.35 <sup>a</sup>	0.34 $\pm$ 0.01 <sup>ab</sup>	0.58 $\pm$ 0.04 <sup>ab</sup>
N-3wR	18.32 $\pm$ 0.87 <sup>a</sup>	0.38 $\pm$ 0.04 <sup>a</sup>	0.67 $\pm$ 0.08 <sup>ab</sup>	25.34 $\pm$ 0.53 <sup>ab</sup>	0.38 $\pm$ 0.01 <sup>ab</sup>	0.60 $\pm$ 0.02 <sup>ab</sup>
N-2wSC	25.01 $\pm$ 1.42 <sup>abcd</sup>	0.27 $\pm$ 0.02 <sup>bcd</sup>	0.38 $\pm$ 0.03 <sup>bcd</sup>	27.37 $\pm$ 1.38 <sup>ab</sup>	0.29 $\pm$ 0.02 <sup>abcd</sup>	0.45 $\pm$ 0.03 <sup>bcd</sup>
N-3wSC	30.20 $\pm$ 1.42 <sup>abcde</sup>	0.30 $\pm$ 0.02 <sup>ab</sup>	0.44 $\pm$ 0.04 <sup>bd</sup>	29.05 $\pm$ 1.05 <sup>abcd</sup>	0.26 $\pm$ 0.01 <sup>abcd</sup>	0.50 $\pm$ 0.03 <sup>ab</sup>

All values are expressed as the mean  $\pm$  SE across six rats in each group. One-way analysis of variance and Bonferroni correction were used. <sup>a</sup> $P < 0.05$ , vs C1 and C2 groups; <sup>b</sup> $P < 0.05$ , vs. HP group; <sup>c</sup> $P < 0.05$ , vs. N-2wR group; <sup>d</sup> $P < 0.05$ , vs. N-2wSC group; <sup>e</sup> $P < 0.05$ , vs N-3wSC group. Control group 1 (C1): Dorsal subcutaneous injection of distilled water (0.1 mL/100 g body weight) for 21 days, followed by sacrifice by decapitation. Control group 2 (C2): Dorsal subcutaneous injection of distilled water (0.1 mL/100 g body weight) for 14 days, followed by no intervention for 4 weeks. Hypoxic (HP) group: Subcutaneous injection of NaNO<sub>2</sub> (35 mg/kg/d) for 21 days. N-2wR and N-3wR groups: subcutaneous injection of NaNO<sub>2</sub> (35 mg/kg/d) for 15 and 21 days respectively, followed by no intervention for 28 and 21 days respectively. N-2wSC group: Subcutaneous injection of NaNO<sub>2</sub> (35 mg/kg/d) for 15 days, followed by one intravenous injection of MSCs *via* the tail vein ( $2 \times 10^6$  cells/rat) and no injection for 28 days. N-3wSC group: Subcutaneous injection of NaNO<sub>2</sub> (35 mg/kg/d) for 15 days, followed by one intravenous injection of MSCs ( $2 \times 10^6$  cells/rat), 7-day NaNO<sub>2</sub> injection, and 21-day no intervention. ATP: Adenosine triphosphate; AMP: adenosine monophosphate.

**Table 4 Levels of NE, DA, and 5-HT levels ( $\mu\text{g/g}$  wet tissue) in the rat cortex and midbrain in each group**

Group	Cortex			Midbrain		
	NE	DA	5-HT	NE	DA	5-HT
C1	0.60 $\pm$ 0.01	1.72 $\pm$ 0.45	0.51 $\pm$ 0.02	0.53 $\pm$ 0.01	1.48 $\pm$ 0.04	0.50 $\pm$ 0.03
C2	0.60 $\pm$ 0.01	1.80 $\pm$ 0.17	0.55 $\pm$ 0.03	0.52 $\pm$ 0.01	1.55 $\pm$ 0.15	0.45 $\pm$ 0.03
HP	0.83 $\pm$ 0.01 <sup>a</sup>	0.86 $\pm$ 0.07 <sup>a</sup>	0.72 $\pm$ 0.02 <sup>a</sup>	0.77 $\pm$ 0.02 <sup>a</sup>	0.91 $\pm$ 0.07 <sup>a</sup>	0.63 $\pm$ 0.02 <sup>a</sup>
N-2wR	0.65 $\pm$ 0.05 <sup>b</sup>	1.18 $\pm$ 0.05 <sup>ab</sup>	0.68 $\pm$ 0.04 <sup>a</sup>	0.60 $\pm$ 0.03 <sup>b</sup>	1.19 $\pm$ 0.05 <sup>ab</sup>	0.55 $\pm$ 0.03 <sup>a</sup>
N-3wR	0.76 $\pm$ 0.07 <sup>ac</sup>	0.91 $\pm$ 0.06 <sup>ac</sup>	0.71 $\pm$ 0.02 <sup>a</sup>	0.65 $\pm$ 0.06 <sup>ab</sup>	0.80 $\pm$ 0.07 <sup>ac</sup>	0.59 $\pm$ 0.04 <sup>a</sup>
N-2wSC	0.58 $\pm$ 0.03 <sup>bd</sup>	1.35 $\pm$ 0.06 <sup>abd</sup>	0.54 $\pm$ 0.01 <sup>bc</sup>	0.53 $\pm$ 0.03 <sup>bd</sup>	1.37 $\pm$ 0.06 <sup>bd</sup>	0.45 $\pm$ 0.01 <sup>bcd</sup>
N-3wSC	0.59 $\pm$ 0.02 <sup>bd</sup>	1.01 $\pm$ 0.04 <sup>ae</sup>	0.58 $\pm$ 0.03 <sup>bc</sup>	0.58 $\pm$ 0.02 <sup>b</sup>	1.04 $\pm$ 0.04 <sup>ade</sup>	0.47 $\pm$ 0.03 <sup>bcd</sup>

All values are expressed as the mean  $\pm$  SE across six rats in each group. One-way analysis of variance and Bonferroni correction were used. <sup>a</sup> $P < 0.05$ , vs. C1 and C2 groups; <sup>b</sup> $P < 0.05$ , vs. HP group; <sup>c</sup> $P < 0.05$ , vs. N-2wR group; <sup>d</sup> $P < 0.05$ , vs. N-2wSC group; <sup>e</sup> $P < 0.05$ , vs. N-3wSC group. Control group 1 (C1): Dorsal subcutaneous injection of distilled water (0.1 mL/100 g body weight) for 21 days, followed by sacrifice by decapitation. Control group 2 (C2): Dorsal subcutaneous injection of distilled water (0.1 mL/100 g body weight) for 14 days, followed by no intervention for 4 weeks. Hypoxic (HP) group: Subcutaneous injection of NaNO<sub>2</sub> (35 mg/kg/d) for 21 days. N-2wR and N-3wR groups: subcutaneous injection of NaNO<sub>2</sub> (35 mg/kg/d) for 15 and 21 days respectively, followed by no intervention for 28 and 21 days respectively. N-2wSC group: Subcutaneous injection of NaNO<sub>2</sub> (35 mg/kg/d) for 15 days, followed by one intravenous injection of MSCs *via* the tail vein ( $2 \times 10^6$  cells/rat) and no injection for 28 days. N-3wSC group: Subcutaneous injection of NaNO<sub>2</sub> (35 mg/kg/d) for 15 days, followed by one intravenous injection of MSCs ( $2 \times 10^6$  cells/rat), 7-day NaNO<sub>2</sub> injection, and 21-day no intervention. NE: Norepinephrine; DA: dopamine; 5-HT: serotonin.

be evidenced by decreased MDA, NO, 8-OHdG, GSSG levels and oxidized GSSG ratio, and increased GSH level and GSH/GSSG ratio. Oxidative stress markers in brain tissue were suppressed by MSCs due to a broad variety of cytokines, chemokines, and growth factors that may potentially be involved in tissue repair introduced by MSCs (Caplan and Dennis, 2006). Findings from this study are consistent with an earlier study (Castorina et al., 2015) that reported the ameliorative effect of MSCs on oxidative stress in neurodegenerative diseases. Oxidative stress markers were neutralized through Nrf2 signalling which might up-regulate the expression of certain anti-apoptotic genes (Levonen et al., 2007). MSCs reduced lipid peroxidation and the levels of oxidative stress markers through activating the enzymatic antioxidant system, or free radical-trapping stimulated by cytokine activation can prevent against brain damage and improve the clinical outcome (Kofman et al., 2012). Exposure to hypoxia results in metabolic failures, such as deple-

tion of ATP stores, enhanced anaerobic glycolysis, activation of calcium-stimulated enzymes, mitochondrial dysfunction, and induced formation of ROS that induces tissue damage (Sims and Anderson, 2002; Endres et al., 2004). The toxicity of nitrite arises from the formation of N-nitroso compounds. The acute toxic effect of nitrite moiety occurs through its ability to oxidize the oxyhemoglobin to methemoglobin, a substance that interferes with the ability of blood cells to carry oxygen in the body (Ger et al., 1996). Hypoxia induced mitochondrial damage leads to severe ATP depletion, thus compromising ionic balance, neuronal signalling, and other vital processes (Hata et al., 2000; Diemel and Hertz, 2005). ATP depletion induces loss of mitochondrial membrane potential, which initiates both apoptotic and necrotic mechanisms of cell death (Gottlieb et al., 2003; Honda et al., 2005). The present results were consistent with the findings of a previous study that reported that exposure to hypoxia decreased cell energy, mainly ATP production,

and increased the level of their metabolites ADP and AMP (Abdel-Rahman et al., 2010). Results of the present studies provide evidence that brain cell energy diminished from the hypoxic brain tissue soon after NaNO<sub>2</sub> administration. In the present study, ATP was decreased and its metabolite ratios were increased readily after NaNO<sub>2</sub> administration. MSCs increased brain cell energy by increasing ATP content and decreasing its metabolite ratios. Recuperating the brain cell energy by MSCs treatment may be due to the “rescue” and possible “replacement” of cells in the lesion tissue (Ruff et al., 2012). Hypoxia is a type of oxidative stress associated with the generation of ROS. This has been suggested to play an important role in the pathogenesis and monoamines depletion (Ahmed-Farid et al., 2016). Hypoxic conditions increase extracellular levels of monoamine neurotransmitters in the brain, and accumulation of NE and 5-HT may influence the development of neuronal death during hypoxia (Akiyama et al., 1991; Hiramatsu et al., 1996). Loss of mitochondrial potential has been shown to be a key event in the demise of neuronal monoamine reuptake under hypoxic conditions (Juurlink and Hertz, 1993). In the present study, in the HP group, DA level in the rat cortex and midbrain was significantly decreased, and NE and 5-HT levels in the rat cortex and midbrain were significantly increased. These results are consistent with the findings of previous studies (Vreman et al., 1998; Omaye, 2002). After NaNO<sub>2</sub> administration, NE and 5-HT levels in the cortex and midbrain were significantly increased, which occurred possibly because of increased NO level. This elevation acts as a vasodilator by binding to soluble guanylate cyclase and modulating its activity by opening Ca-activated-K channels (Ischiropoulos et al., 1996). MSCs have the ability to generate neurons and glia within the brain. Therefore, more researches are undertaken to develop methods and techniques in which stem cells grown in culture can be implanted into patient’s brains where stem cells are able to be transformed into neurons and glia, and to determine a mechanism by which the differentiated neurons and glial cells can be implanted (Temple, 2001). Results from this study showed that the repair process of damaged neurons by MSCs, in particular neurotransmitter depletion, was achieved by stimulating the sub-thalamic nucleus or the internal segment of the globus pallidus (Perlmutter and Mink, 2006). Accordingly, stem cells can activate neurons to release monoamines such as NE, DA, and 5-HT which were degenerated by different models. Moreover, Parkinson’s disease (PD) is caused by a progressive degeneration and loss of dopamine (DA)-producing neurons, which leads to tremor, rigidity, and hypokinesia (abnormally decreased mobility). MSCs can be differentiated into DA neurons by introducing the gene *Nurr1*. The MSCs transplanted into the brain of a rat model of PD can improve rat motor function by MSCs-derived DA neurons releasing DA (Chung et al., 2002). Oxyhemoglobin oxidizes to methemoglobin by sodium nitrite and also produces NO<sub>2</sub> and NO<sub>3</sub>. Nitric oxide binds with hemoglobin reversibly and gradually that auto-decreases to HbFe<sup>2+</sup>. Moreover, NO<sub>2</sub> reversibly unites with methemoglobin which produces a mixture of compounds. Overall, these reactions place the biological system in oxidative stress causing apoptosis. This

mechanism supports results and findings with sodium nitrite administration in rats. Feelisch and Noack reported dangerous effects of the extreme use of nitrites indicating an important threat for the composition and/or role in neuronal tissues (Feelisch and Noack, 1987). This supports the results of a study by Zadnipyryany and Sataieva (2014) who found that rats treated by NaNO<sub>2</sub> for 3 weeks exhibited dilated capillary blood vessels, lymphocytic inflammatory cells, damaged pia mater with hemorrhagic change, loss of plexus, necrotic areas with pyknotic nuclei, and widely distributed large vacuoles in the hypoxic cerebral cortex. Zhu et al. (2003) reported that the mitochondria participate in the cell death process through liberating various pro-apoptotic proteins like caspase-2 and -9, cytochrome, and AIF from the inter membrane space. Caspase-3, BAX and caspase-12 are considered the key components of apoptosis and are upregulated in the developing brain. Inadequate transportation of oxygen and nutrients to the immature brain endangers the function of the brain throughout the whole lifespan as one of the main reasons for neurodegenerative alternation and pathogenesis of the tissue organs. This finding is consistent with a previous study (Zadnipyryany and Sataieva, 2014). In the present study, hyperplasia of astrocytes in the cerebral tissue and capillary blood vessels was observed. Absorption of blood cells may lead to the formation of small vacuoles, which is related to secondary brain injury that is triggered by neutrophil infiltration. These results are consistent with the findings of a previous study (Miao et al., 2012). Oxygen is required to generate energy; cells make ATP from lipids as the next supply for energy creation. Fatty droplets form as a consequence of metabolism of lipids. Lipid vacuoles form as a result of lipid peroxidation and oxidative stress in the brain. Hypoxia occurs when cerebral blood flow in the brain is disturbed. It limits the transportation of substrates, principally glucose and oxygen, and damages the necessary energetics to preserve ionic gradients. The membrane potential is damaged with energy malfunction, and the neurons and glia lose their polarities. Then, the voltage dependent Ca<sup>2+</sup> channels become triggered and induce accumulation of free Ca<sup>2+</sup> intra-neuron (Acker and Acker, 2010).

Stem cell therapy was introduced to repair capillary damage in the developing brain. Epithelial-derived cells in rats treated for 2 and 3 weeks with NaNO<sub>2</sub>, and treated with stem cells, lead to more ameliorative cerebral tissue nearly similar to normal tissue. Stem cells defend against infection and liberate five growth factors, and so MSCs are able to differentiate and then repair the injured tissues. After oxygenation and cerebral perfusion return, hypoxia-caused cytotoxic oedema and gathering of excitatory amino acids are regularly normalized, collectively with improvement of the metabolic dysfunction of the brain (Gunn and Thoresen, 2006). These findings parallel with our investigations. Ki67 and proliferating cell nuclear antigen (PCNA) are two indicators used to identify cell proliferation. Ki67 is a nuclear protein that is synthesized in G1, S, G2, and M phases in the cell cycle; however, its role is not known (Kee et al., 2002). PCNA is a nuclear protein which is expressed in the phases G1 and S of the cell cycle. The present results are consistent with those of the previous study (Raucci et al., 2006). The PCNA-immunoreactive cell number change in rat brains indicates various actions of different kinds of



brain cells and controls the equilibrium among cell apoptosis and proliferation (Zhou et al., 2014).

Rats treated for 2 weeks by NaNO<sub>2</sub> and left for recovery for one month exhibited ameliorative cerebral tissue. This supports the findings of the previous study (Parr et al., 2007) which demonstrated that transplantation of MSCs improved the histopathological changes of injured brain tissue, promoted brain tissue repair, and contributed to brain function recovery. However, the biological origin of neurogenesis caused by hypoxia remains poorly understood and requires further investigation. The main obstruction limiting the clinical application of MSCs is the deficiency of defined markers, because of the natural heterogeneity of MSCs and dissimilarity linked with cell processing and spreading (Ma, 2010). Hypoxia influences cellular actions, cytokine functioning, and regenerative potential, and could actually be an “*in situ*” normal level (Ivanovic, 2009). Although hypoxia has been documented as a developmentally significant stimulus *in vivo*, it has not been sufficiently studied *in vitro* (Ma, 2009). MSCs healing properties are currently well-recognized not only by their widespread differentiation but also their capacity to take action and manipulate their direct close surroundings.

In conclusion, rats exposed to NaNO<sub>2</sub> at different time intervals have impaired antioxidant enzyme, non-enzyme, brain cell energy, and brain monoamines depletion compared with controls, and MSCs therapy improved these findings. This suggests that MSCs alleviated brain injury induced by hypoxia and stimulated the antioxidant defence to promote neuron function and nervous system performance. Histological results revealed that stem cells prevented against neurotoxicity due to hypoxic NaNO<sub>2</sub> effects on rat brain, and improved the pathological features of neurodegenerative disorders. Results from the study of PCNA-immunoreactive cells suggest that MSCs may differentiate into glial cells and neurons. The stem cell therapy holds promise for the treatment of a wide range of neurological disorders. As the number and type of regenerative cells have not been identified in this study, future studies are required. Additionally, an *in vitro* study should be required to confirm the differentiation of stem cells into glial or neuronal cells.

**Acknowledgments:** The authors would like to acknowledge Professor Laila A. Rashed, from Faculty of Medicine, Cairo University, Egypt, for providing the MSCs for the experiments and the fluorescence microscopy images of homing cells.

**Author contributions:** All authors participated in conception and design of the study, analyzed and interpreted the data, drafted the paper, and approved the final version of this paper.

**Conflicts of interest:** None declared.

**Research ethics:** The protocol for the conducted animal experiments was approved by the Research Ethics Committee of the Faculty of Women for Art, Sciences and Education, Ain Shams University, Cairo, Egypt which followed the recommendations in the *Guide for the Care and Use of Laboratory Animals of the National Institutes of Health (NIH publication no. 85-23, revised 1996)*.

**Data sharing statement:** Datasets analyzed during the current study are available from the corresponding author on reasonable request.

**Plagiarism check:** Checked twice by iThenticate.

**Peer review:** Externally peer reviewed.

**Open access statement:** This is an open access article distributed under the terms of the Creative Commons Attribution-NonCommercial-ShareAlike 3.0 License, which allows others to remix, tweak, and build upon the work non-commercially, as long as the author is credited and the

new creations are licensed under identical terms.

## References

- Abdel-Rahman M, Shehata AM, Elsisy SF, Haridy SA (2010) Study on the protective effect of methylene blue against the neurological toxicity of carbon monoxide in adult female albino rats. *Med J Cairo Univ* 78:259-268.
- Acker T, Acker H (2010) Cellular oxygen sensing need in CNS function: physiological and pathological implications. *J Exp Biol* 207:3171-3188.
- Ahmed-Farid OA, Ahmed RF, Saleh DS (2016) Combination of resveratrol and fluoxetine in an acute model of depression in mice: Prevention of oxidative DNA fragmentation and monoamines degradation. *J Appl Pharm Sci* 6:1-7.
- Aita NA, Mohammed FF (2014) Effect of marjoram oil on the clinicopathological, cytogenetic and histopathological alterations induced by sodium nitrite toxicity in rats. *Glob Vet* 12:606-616.
- Akiyama Y, Koshimura K, Ohue T, Lee K, Miwa S, Yamagata S, Kikuchi H (1991) Effects of hypoxia on the activity of the dopaminergic neuron system in the rat striatum as studied by *in vivo* brain microdialysis. *J Neurochem* 57:997-1002.
- Alhadlaq A, Mao JJ (2004) Mesenchymal stem cells: isolation and therapeutics. *Stem Cells Dev* 13:436-448.
- Bancroft JD, Cook HC, Turner DR (1994) Immunocytochemistry. In: *Manual of histological techniques and their diagnostic applications*. 2nd ed. London Churchill Livingstone.
- Barnham KJ, Masters CL, Bush AI (2004) Neurodegenerative diseases and oxidative stress. *Nat Rev Drug Discov* 3:205-214.
- Bhanumathy M, Harish MS, Shivaprasad HN, Sushma G (2010) Nootropic activity of *Celastrus paniculatus* seed. *Pharm Biol* 48:324-327.
- Blomgren K, Zhu C, Wang X, Karlsson JO, Leverin AL, Bahr BA, Mallard C, Hagberg H (2001) Synergistic activation of caspase-3 by m-calpain after neonatal hypoxia-ischemia: a mechanism of “pathological apoptosis”? *J Biol Chem* 276:10191-10198.
- Caplan AI, Dennis JE (2006) Mesenchymal stem cells as trophic mediators. *J Cell Biochem* 98:1076-1084.
- Castorina A, Szychlińska MA, Marzagalli R, Musumeci G (2015) Mesenchymal stem cells-based therapy as a potential treatment in neurodegenerative disorders: is the escape from senescence an answer? *Neural Regen Res* 10:850-858.
- Chung S, Sonntag KC, Andersson T, Bjorklund LM, Park JJ, Kim DW, Kang UJ, Isacson O, Kim KS (2002) Genetic engineering of mouse embryonic stem cells by Nurr1 enhances differentiation and maturation into dopaminergic neurons. *Eur J Neurosci* 16:1829-1838.
- Craun GF, Greathouse DG, Gunderson DH (1981) Methaemoglobin levels in young children consuming high nitrate well water in the United States. *Int J Epidemiol* 10:309-317.
- Dienel GA, Hertz L (2005) Astrocytic contributions to bioenergetics of cerebral ischemia. *Glia* 50:362-388.
- Drury RB, Wallington EA (1980) *Carleton's Histological Technique*, 5th ed. Oxford University.
- El-Sheikh NM, Khalil FA (2011) L-Arginine and L-glutamine as immunonutrients and modulating agents for oxidative stress and toxicity induced by sodium nitrite in rats. *Food Chem Toxicol* 49:758-762.
- Endres M, Biniszkievicz D, Sobol RW, Harms C, Ahmadi M, Lipski A, Katchanov J, Mergenthaler P, Dirnagl U, Wilson SH, Meisel A, Jaenisch R (2004) Increased postischemic brain injury in mice deficient in uracil-DNA glycosylase. *J Clin Invest* 113:1711-1721.
- Farias JG, Bustos-Obregón E, Orellana R, Bucarey JL, Quiroz E, Reyes JG (2005) Effects of chronic hypobaric hypoxia on testis histology and round spermatid oxidative metabolism. *Andrologia* 37:47-52.
- Feelisch M, Noack E (1987) Nitric oxide (NO) formation from nitrovasodilators occurs independently of hemoglobin or non-heme iron. *Eur J Pharmacol* 142:465-469.
- Fellman V, Raivio AK (1997) Reperfusion injury as the mechanism of brain damage after perinatal asphyxia. *Pediatr Res* 41:599-606.
- Ger J, Kao H, Shih TS, Deng JF (1996) Fatal toxic methemoglobinemia due to occupational exposure to methyl nitrite. *Clin Med J* 57:578.
- Gottlieb E, Armour SM, Harris MH, Thompson CB (2003) Mitochondrial membrane potential regulates matrix configuration and cytochrome c release during apoptosis. *Cell Death Differ* 10:709-717.
- Gunn AJ, Thoresen M (2006) Hypothermic neuroprotection. *NeuroRx* 3:154-169.

- Hata R, Maeda K, Hermann D, Mies G, Hossmann KA (2000) Evolution of brain infarction after transient focal cerebral ischemia in mice. *J Cereb Blood Flow Metab* 20:937-946.
- Hiramatsu M, Kameyama T, Nabeshima T (1996) Carbon monoxide-induced impairment of learning, memory and neuronal dysfunction. In: Penney DG (ed). *Carbon Monoxide*. CRC Press: Boca Raton, FL.
- Honda HM, Korge P, Weiss JN (2005) Mitochondria and ischemia/reperfusion injury. *Ann N Y Acad Sci* 1047:248-258.
- Ischiropoulos H, Beers MF, Ohnishi ST, Fisher D, Garner SE, Thom SR (1996) Nitric oxide production and perivascular tyrosine nitration in brain after carbon monoxide poisoning in the rat. *J Clin Invest* 97:2260-2267.
- Ivanovic Z (2009) Hypoxia or in situ normoxia: The stem cell paradigm. *J Cell Physiol* 219:271-275.
- Jaiswal N, Haynesworth SE, Caplan AL, Bruder SP (1997) Osteogenic differentiation of purified, culture-expanded human mesenchymal stem cells in vitro. *J Cell Biochem* 64:295-312.
- Jayatilake E, Shaw S (1993) A high performance liquid chromatographic assay for reduced and oxidized glutathione in biological samples. *Anal Biochem* 214:452-457.
- Juurlink BH, Hertz L (1993) Ischemia-induced death of astrocytes and neurons in primary culture: pitfalls in quantifying neuronal cell death. *Brain Res Dev Brain Res* 71:239-246.
- Karatas F, Karatepe M, Baysar A (2002) Determination of free malondialdehyde in human serum by high performance liquid chromatography. *Anal Biochem* 311:76-79.
- Karatepe M (2004) Simultaneous determination of ascorbic acid and free malondialdehyde in human serum by HPLC-UV. *LC GC N Am* 22:362-365.
- Kee N, Sivalingam S, Boonstra R, Wojtowicz JM (2002) The utility of Ki-67 and BrdU as proliferative markers of adult neurogenesis. *J Neurosci Methods* 115:97-105.
- Kim SU, de Vellis J (2009) Stem cell-based cell therapy in neurological diseases: a review. *J Neurosci Res* 87:2183-2200.
- Knobeloch L, Salna B, Hogan A, Postle J, Anderson H (2000) Blue babies and nitrate-contaminated well water. *Environ Health Perspect* 108:675-678.
- Kofman AE, McGraw MR, Payne CJ (2012) Rapamycin increases oxidative stress response gene expression in adult stem cells. *Aging (Albany NY)* 4:279-289.
- Kosaka H, Imaizumi K, Imai K, Tyuma I (1979) Stoichiometry of the reaction of oxyhemoglobin with nitrite. *Biochim Biophys Acta* 581:184-188.
- Kovács P, Juránek I, Stankovicová T, Svec P (1996) Lipid peroxidation during acute stress. *Pharmazie* 51:51-53.
- Lan KM, Tien LT, Cai Z, Lin S, Pang Y, Tanaka S, Rhodes PG, Bhatt AJ, Savich RD, Fan LW (2016) Erythropoietin ameliorates neonatal hypoxia-ischemia-induced neurobehavioral deficits, neuroinflammation, and hippocampal injury in the juvenile rat. *Int J Mol Sci* 17:289.
- Lee JS, Hong JM, Moon GJ, Lee PH, Ahn YH, Bang OY; STARTING collaborators (2010) A long-term follow-up study of intravenous autologous mesenchymal stem cell transplantation in patients with ischemic stroke. *Stem Cells* 28:1099-1106.
- Levonen AL, Inkala M, Heikura T, Jauhiainen S, Jyrkkänen HK, Kansanen E, Määttä K, Romppanen E, Turunen P, Rutanen J, Ylä-Herttua S (2007) Nrf2 gene transfer induces antioxidant enzymes and suppresses smooth muscle cell growth in vitro and reduces oxidative stress in rabbit aorta in vivo. *Arterioscler Thromb Vasc Biol* 27:741-747.
- Liu J, Wang X, Shigenaga MK, Yeo HC, Mori A, Ames BN (1996) Immobilization stress causes oxidative damage to lipid, protein, and DNA in the brain of rats. *FASEB J* 10:1532-1538.
- Lodovici M, Casalini C, Briani C, Dolara P (1997) Oxidative liver DNA damage in rats treated with pesticide mixtures. *Toxicology* 117:55-60.
- Ma T (2010) Mesenchymal stem cells: From bench to bedside. *World J Stem Cells* 2:13-17.
- Ma T, Grayson WL, Fröhlich M, Vunjak-Novakovic G (2009) Hypoxia and stem cell-based engineering of mesenchymal tissues. *Biotechnol Prog* 25:32-42.
- Miao X, Liu X, Yue Q, Qiu N, Huang W, Wang J, Xu Y, Zhang Y, Yang J, Chen X (2012) Deferoxamine suppresses microglia activation and protects against secondary neural injury after intracerebral hemorrhage in rats. *Nan Fang Yi Ke Da Xue Xue Bao* 32:970-975.
- Moisan A, Pannetier N, Grillon E, Richard MJ, de Fraipont F, Rémy C, Barbier EL, Detante O (2012) Intracerebral injection of human mesenchymal stem cells impacts cerebral microvasculature after experimental stroke: MRI study. *NMR Biomed*. 2012 Dec;25(12):1340-8.
- Omaye ST (2002) Metabolic modulation of carbon monoxide toxicity. *Toxicology* 180:139-150.
- Page P, Blome J, Wolf HU (2000) High-performance liquid chromatographic separation and measurement of various biogenic compounds possibly involved in the pathomechanism of Parkinson's disease. *J Chromatogr B Biomed Sci Appl* 746:297-304.
- Papadoyannis LN, Samanidou VF, Nitsos CC (1999) Simultaneous determination of nitrite and nitrate in drinking water and human serum by high performance anion-exchange chromatography and UV detection. *J Liq Chromatogr Relat Technol* 22:2023-2041.
- Parr AM, Tator CH, Keating A (2007) Bone marrow-derived mesenchymal stromal cells for the repair of central nervous system injury. *Bone Marrow Transplant* 40:609-619.
- Perlmutter JS, Mink JW (2006) Deep brain stimulation. *Annu Rev Neurosci* 29:229-257.
- Raucci F, Di Fiore MM, Pinelli C, D'Aniello B, Luongo L, Polese G, Rastogi RK (2006) Proliferative activity in the frog brain: a PCNA-immunohistochemistry analysis. *J Chem Neuroanat* 32(2-4):127-142.
- Roland EH, Hill A, Norman MG, Flodmark O, MacNab AJ (1988) Selective brainstem injury in an asphyxiated newborn. *Ann Neurol* 23:89-92.
- Ruff CA, Wilcox JT, Fehlings MG (2012) Cell-based transplantation strategies to promote plasticity following spinal cord injury. *Exp Neurol* 235:78-90.
- Salama MF, Abbas A, Darweish MM, El-Hawwary AA, Al-Gayyar MM (2013) Hepatoprotective effects of cod liver oil against sodium nitrite toxicity in rats. *Pharm Biol* 51:1435-1443.
- Sataieva TP, Zadnipyany IV (2015) Hypoxic damage of cardiomyocytes during pregnancy and its experimental treatment. *Int Stud J Med* 1:18-21.
- Semenza GL (2002) Signal transduction to hypoxia-inducible factor 1. *Biochem Pharmacol* 64:993-998.
- Seo MS, Jeong YH, Park JR, Park SB, Rho KH, Kim HS, Yu KR, Lee SH, Jung JW, Lee YS, Kang KS (2009) Isolation and characterization of canine umbilical cord blood-derived mesenchymal stem cells. *J Vet Sci* 10:181-187.
- Sims NR, Anderson MF (2002) Mitochondrial contributions to tissue damage in stroke. *Neurochem Int* 40:511-526.
- Smith RP (1967) The nitrite methemoglobin complex its significance in methemoglobin analyses and its possible role in methemoglobinemia. *Biochem Pharmacol* 16:1655-1664.
- Sohni A, Verfaillie CM (2013) Mesenchymal stem cells migration homing and tracking. *Stem Cells Int* 2013:130763.
- Spagnuolo C, Rinnelli P, Coletta M, Chiancone E, Ascoli F (1987) Oxidation reaction of human oxyhemoglobin with nitrite: a reexamination. *Biochim Biophys Acta* 911:59-65.
- Teerlink T, Hennekes M, Bussemaker J, Groeneveld J (1993) Simultaneous determination of creatine compounds and adenine nucleotides in myocardial tissue by high-performance liquid chromatography. *Anal Biochem* 214:278-283.
- Temple S (2001) The development of neural stem cells. *Nature* 414:112-117.
- Vremar HJ, Wong RJ, Sanesi CA, Dennery PA, Stevenson DK (1998) Simultaneous production of carbon monoxide and thiobarbituric acid reactive substances in rat tissue preparations by an iron-ascorbate system. *Can J Physiol Pharmacol* 76:1057-1065.
- Yu B, Meng F, Yang Y, Liu D, Shi K (2016) NOX2 antisense attenuates hypoxia-induced oxidative stress and apoptosis in cardiomyocyte. *Int J Med Sci* 13:646-652.
- Zadnipyany IV, Sataieva TP (2014) Neonatal rat myocardium survival in terms of chronic hemic hypoxia. *World Sci Discov* 10:281-290.
- Zhang J, Piantadosi CA (1992) Mitochondrial oxidative stress after carbon monoxide hypoxia in rat brain. *J Clin Invest* 90:1193-1199.
- Zhou L, Deng L, Chang NB, Dou L, Yang CX (2014) Cell apoptosis and proliferation in rat brains after intracerebral hemorrhage: role of Wnt/ $\beta$ -catenin signaling pathway. *Turk J Med Sci* 44:920-927.
- Zhu C, Qiu L, Wang X, Hallin U, Candé C, Kroemer G, Hagberg H, Blomgren K (2003) Involvement of apoptosis-inducing factor in neuronal death after hypoxia-ischemia in the neonatal rat brain. *J Neurochem* 86:306-317.